Science and Technology Indonesia
e-ISSN:2580-4391 *p*-ISSN:2580-4405
Vol. 7, No. 4, October 2022

Research Paper

Variation of M^{2+} (Ni and Zn) in Cellulose-based M^{2+}/Cr Composite Materials to Determine Adsorption and Regeneration Abilities on Phenol Removal

Alfan Wijaya[1], Tarmizi Taher[2,4], Aldes Lesbani[3,4], Risfidian Mohadi[1,4]*

[1]*Magister Programme Graduate School of Mathematics and Natural Sciences, Sriwijaya University, Palembang, 30139, South Sumatera, Indonesia*
[2]*Department of Environmental Engineering, Faculty of Mathematics and Natural Sciences, Institut Teknologi Sumatera, Lampung, 35365, Indonesia*
[3]*Graduate School of Mathematics and Natural Sciences, Sriwijaya University, Palembang, 30139, Indonesia*
[4]*Research Centre of Inorganic Materials and Coordination Complexes, Faculty of Mathematics and Natural Sciences, Sriwijaya University, Palembang, 30139, South Sumatera, Indonesia*
***Corresponding author**: risfidian.mohadi@unsri.ac.id

Abstract
Cellulose-based Ni/Cr (Ni/Cr-C) and cellulose-based Zn/Cr (Zn/Cr-C) composite materials have been successfully carried out, which is indicated by the XRD, FTIR, and BET analysis. Layered double hydroxide Ni/Cr (Ni/Cr-LDH) increased surface area from 0.128 m^2/g to 2.207 m^2/g in Ni/Cr-C composites, and layered double hydroxide Zn/Cr (Zn/Cr-LDH) also increased surface area from 0.133 m^2/g to 3.714 m^2/g in Zn/Cr-C composites. The pHpzc of the material in this study is pH 5.94-8.43, while the optimum pH of all materials is pH 9. Ni/Cr-LDH experienced an increase in adsorption capacity after becoming a Ni/Cr-C composite, from 8.985 mg/g to 24.510 mg/g, and Zn/Cr-LDH experienced an increase in adsorption capacity from 13.263 mg/g to 30.960 mg/g in Zn/Cr-C. Zn/Cr-C composite material has a greater adsorption ability than Ni/Cr-C. Kinetic and isotherm model in this study followed by PSO kinetic with optimum contact time at 70 minutes and Freundlich isotherm. Ni/Cr-C and Zn/Cr-C composite materials can be used repeatedly in the regeneration process until the 4^{th} cycle.

Keywords
LDH, Cellulose, Composites, Adsorption, Phenol, Regeneration

Received: 21 July 2022, Accepted: 10 October 2022
https://doi.org/10.26554/sti.2022.7.4.461-468

1. INTRODUCTION

Layered double hydroxide (LDH) is one of the layered materials which have a general structure $[M^{2+}{}_{1-x}\ M^{3+}x\ (OH)_2]^{2+}[A^{n-}x/n.\ m\ H_2O]$ with excellent ion exchange capacity, large specific surface area, controllable morphology, and electropositive surface, making LDH a suitable material for adsorption of organic pollutants, cationic or anionic dyes, antibiotic molecules, and heavy metal ions (Wang et al., 2022; Yuliasari, 2022). However, the layered double hydroxide structure is less stable and the layer is easily peeled off during the repeated use process. This material allows it to be modified to be used repeatedly and improve performance. One way of modification is by composting with carbon-based materials such as cellulose. Based on research conducted by Sun et al. (2022), cellulose/MgAl composites layered double hydroxides (LDHs) have a high specific surface area which is beneficial for the adsorption process. Cellulose also has a large pore structure and includes green and eco-friendly adsorbents.

This study used composite materials to remove phenols, including harmful organic pollutants. Phenol is a volatile organic compound (VOC) that is very harmful to the environment, humans, and other living things even at low concentrations of less than 1.0 μg/L because it is highly toxic and carcinogenic. Phenols are found in many sources such as the petrochemical industry, medical wastewater, coal conversion, wood products, paint, pesticides, and paper industries (Chaghaganooj et al., 2021; Dong et al., 2021; da Silva et al., 2022; Gao et al., 2022). Therefore, it is important to carry out treatment for the removal of this phenol organic pollutant. phenol removal method in this study using adsorption method. Adsorption method is a widely used technique for managing organic pollutants because it has many advantages such as eco-friendly, economic feasibility, cost-effectiveness, simplicity, flexibility, and high efficiency (Ullah et al., 2022; Sahu et al., 2021; Dehmani et al., 2022).

This study modified the composite material by varying M^{2+} on the composite material cellulose-based M^{2+}/Cr to see the adsorption and regeneration abilities in removing phenol organic pollutants. Juleanti et al. (2021) conducted a study by

varying M^{2+} (Ca and Mg) on M^{2+}/Al-based biochar composite materials which showed differences in adsorption ability, where biochar-based Ca/Al has a greater adsorption capacity compared to biochar-based Mg/Al. Composite materials prepared in this study are proven by characterization data, including XRD, FT-IR, and BET. This research was conducted with several treatments and parameters such as the influence of pH, adsorption contact time, effect of initial concentration and temperature on the adsorption process, isotherm, and thermodynamic parameters.

2. EXPERIMENTAL SECTION

2.1 Chemicals and Instrumentation

The materials used in this study such as $Ni(NO_3)_2.6H_2O$, $Zn(NO_3)_2.6H_2O$, $Cr(NO_3)_3.9H_2O$, distilled water, phenol (C_6H_5OH), 4-amino antipyrine ($C_{11}H_{13}N_3O$), potassium hexacyanoferrate (III) ($K_3[Fe(CN)_6]$), buffer solution pH 10, HCl, and NaOH. The synthesized material was characterized using an X-Ray Rigaku Miniflex-600 diffractometer, Shimadzu Prestige-21 FTIR Spectrophotometer, BET Surface Area Analyzer Micrometric ASAP Quantachrome, and absorbance measurement of solution using Biobase Spectrophotometer UV-Visible BKUV1800PC.

2.2 Synthesis of Ni/Cr-LDH and Zn/Cr-LDH

Synthesis of Ni/Cr-LDH was carried out with $Ni(NO_3)_2.6H_2O$ 0.75 M solution of 100 mL mixed with 100 mL $Cr(NO_3)_3.9H_2O$ 0.25 M. Then added 2 M sodium hydroxide (NaOH) solution slowly up to pH 8 and heated at a temperature of 60°C. Constant stirring was performed for 12 hours at a temperature of 80°C. The obtained precipitate was filtered and washed using aqueous to a neutral pH. The residue was dried for 24 hours using an oven at 60°C. Synthesis of Zn/Cr-LDH was carried out with $Zn(NO_3)_2.6H_2O$ solution of 100 mL mixed with 100 mL $Cr(NO_3)_3.9H_2O$ (ratio molar 2:1), and then a mixture of Na_2CO_3 2.5 M and NaOH 2 M solutions is slowly added to pH 10 and then stirred for 2 hours. The mixture is heated at 60°C for 24 hours. The obtained precipitate was filtered and washed using aqueous to a neutral pH and dried using an oven at 60°C for 24 hours. The synthesized materials were characterized using XRD, FT-IR, and BET analysis.

2.3 Preparation of Ni/Cr-C and Zn/Cr-C Composites

Composite materials were prepared using the method of coprecipitation with a constant pH. A total of 30 mL of $Ni(NO_3)_2.6H_2O$ or $Zn(NO_3)_2.6H_2O$ 0.75 M solution and 30 mL of $Cr(NO_3)_3.9H_2O$ 0.25 M solutions were mixed and set pH to 10 using a solution of NaOH 2 M. The mixture was stirred for 1 hour, then 3 g of cellulose was added. The solution is heated at a temperature of 80°C for 3 days. The precipitate was filtered and dried using the oven at 80°C for 24 hours. The prepared materials were characterized using XRD, FT-IR, and BET analysis.

2.4 Study of pH point zero charge (pHpzc)

The study of pHpzc was performed by adding 0.02 g of adsorbent each to 20 mL of NaCl solution with a concentration of 0.1 M which has been pH-regulated with pH variations of 2, 3, 4, 5, 6, 7, 8, 9, 10, and 11. NaCl solution is pH regulated by adding a solution of NaOH and HCl with a concentration of 0.1 M. The mixture is stirred for 24 hours, then filtering is carried out and the filtrate is measured at the final pH using a pH meter. Determining the pHpzc of each material was carried out by graphing the relationship between the initial pH and the final pH.

2.5 Adsorption Process

The adsorption process in this study was carried out with several treatments, such as the influence of pH, adsorption contact time, and the influence of initial concentration and temperature on the adsorption process. The effect of pH adsorption can be studied by performing a phenol adsorption process on pH variations (2-11) which aims to determine the optimum pH in the adsorption process. As much as 0.02 g adsorbents were added to an Erlenmeyer containing 20 mL of phenol solution with a concentration of 10 mg/L and the mixture was stirred for 2 hours. The effect of contact time adsorption on phenol can be studied by varying the contact time to determine the optimum time. As much as 0.02 g adsorbents were added to an Erlenmeyer containing 20 mL of phenol solution with a concentration of 10 mg/L and the mixture was stirred. The effect of initial concentration and temperature adsorption was studied by varying the concentration (10, 15, 20, 25, and 30 mg/L) and temperature (30, 40, 50, 60, and 70°C). As much as 0.02 g adsorbents were added to an Erlenmeyer containing 20 mL of phenol solution and stirred during the optimum time. The filtrate was measured using a UV-Vis spectrophotometer. The filtrate of the phenol solution was complex first before measuring its absorbance. As much as 1 mL phenol solution was put in a beaker and then a 4-amino antipyrine reagent solution of 2% was added to as much as 0.1 mL, an 8% solution of potassium hexacyanoferrate (III) as much as 0.1 mL, the solution of pH 10 buffer of 1 mL was added and 3 mL was added, then homogenized and allowed to stand for 15 minutes.

2.6 Desorption Process and Study of Regeneration Ability

The desorption process is carried out before the adsorbent regeneration process. The desorption process is performed on adsorbents that have been adsorbents that have been adsorbed phenol by using an ultrasonic system. After the desorption process, the regeneration process was carried out by adding 0.1 g of adsorbent to a phenol solution of 10 mg/L then stirred for 2 hours and the absorbance of the filtrate was measured using a UV-Visible spectrophotometer and adsorbents dried in the oven. The dried adsorbent was carried out in the desorption process, then the regeneration process was carried out for the next cycle.

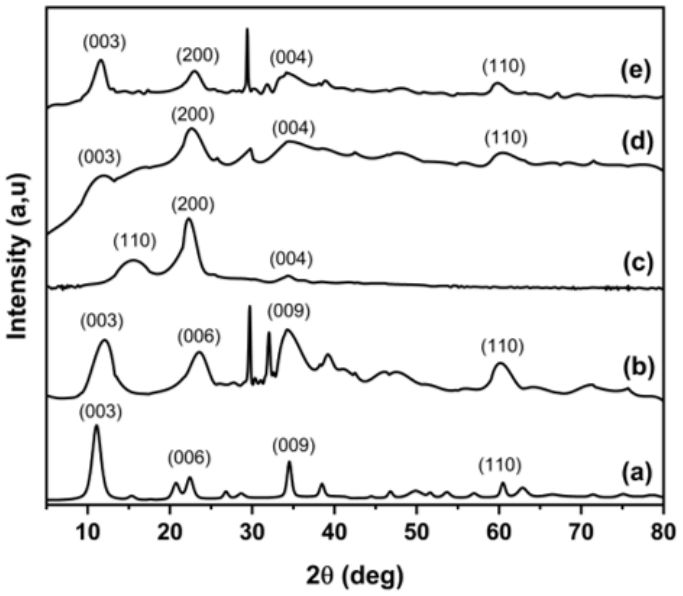

Figure 1. Diffraction patterns of Ni/Cr-LDH (a), Zn/Cr-LDH (b), Cellulose (c), Ni/Cr-C (d), and Zn/Cr-C (e)

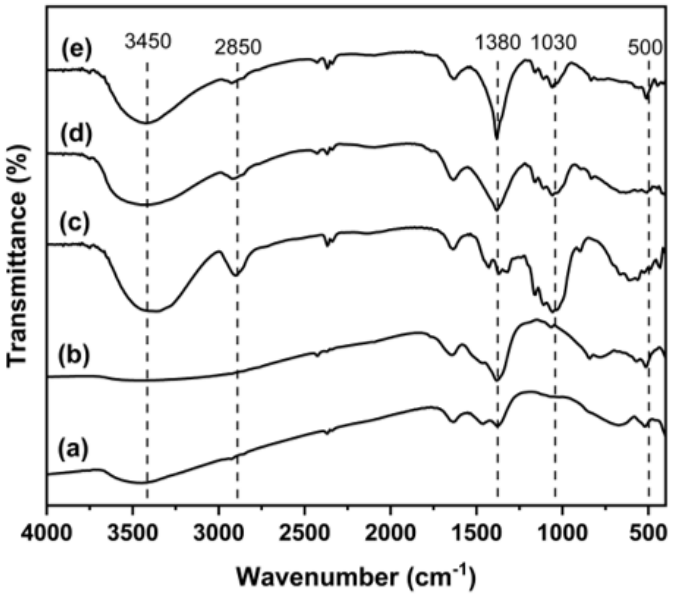

Figure 2. FT-IR Spectrum of Ni/Cr-LDH (a), Zn/Cr-LDH (b), Cellulose (c), Ni/Cr-C (d), and Zn/Cr-C (e)

3. RESULT AND DISCUSSION

The results of the XRD characterization analysis can be seen in Figure 1. Based on figure 1, Ni/Cr-LDH has a diffraction peak at an angle of 11.4° (003), 23.3° (006), 34° (009), and 60.8° (110). Padalkar et al. (2022)) reported that Ni/Cr-LDH had diffraction peaks at angles of 11° (003), 23° (006), and 60° (110) according to JCPDS data (74-1057). Peak diffraction at Zn/Cr-LDH appeared at angles of 11.74° (003), 23.49° (006), 34.33° (009), 39.26° (012) and 60.41° (110) according to JCPDS data (51-1525). According to Liu et al. (2018), typical diffraction peaks at angles of 11° (003) and 22° (006) indicate that the layered double hydroxide material is a layered material. The peaks of diffraction in cellulose shown in Figure 1 appear at angles of 15.19° (110), 22.67° (200), and 34.49° (004) which have similarities to the study conducted by Debnath et al. (2022). The successful modification of layered double hydroxide materials to form LDH-cellulose composites were evidenced by the emergence of layered double hydroxide diffraction peaks and cellulose in composite materials. Ni/Cr-C composites have diffraction peaks at angles of 11° (003) and 60.3° (110) which are typical peaks of Ni/Cr-LDH and peaks at angles of 22.88° (200) known to be characteristics peaks of cellulose. The diffraction peaks that appear on the Zn/Cr-C composite at angles of 11.62° (003) and 59.86 (110) are known to be typical peaks of Zn/Cr-LDH and at an angle of 22.90° (200) are t characteristics peaks of cellulose.

The results of the FT-IR analysis can be seen on the FT-IR spectrum shown in Figure 2. Based on the FT-IR spectra in Figure 2, it can be seen that all materials have widened vibrations in the area of 3500-3200 cm^{-1} which indicates the presence of an -OH group of water molecules. Vibrations that appear in layered double hydroxide materials in the wave number area of 1380 cm^{-1} indicate the presence of an N-O group of nitrates and in regions around 600-700 cm^{-1} indicate the presence of metal bonds with oxygen (M-O). Vibrations that appear in cellulose in regions around 3000-2850 cm^{-1} indicate the presence of aliphatic -CH from alkanes and in areas of 1030 cm^{-1} indicate the presence of a C-O-C group in cellulose. Based on Figure 1, the LDH-cellulose composite material appears to be a typical vibration combined with layered double hydroxide and cellulose materials. The vibration that occurs in the region of about 1380 cm^{-1} (N-O) in the area of about 600-700 cm^{-1} (M-O) is known as a typical vibration of layered double hydroxide, while the vibration that appears in the wave number area 3000-2850 cm^{-1} (-CH aliphatic) and in the area 1030 cm^{-1} (C-O-C) is a typical vibration of cellulose.

Based on the BET analysis data in Figure 3, it can be seen that each material shows a type IV isotherm based on the IUPAC classification with the presence of particles of mesoporous size with hysteresis activity. Hysteresis activity shows the material has non-uniform pores, so that the graph between adsorption and desorption occurs a difference. Based on the data from the measurement results of the BET analysis in Table 1, it can be seen that there is an increase in the surface area of the layered double hydroxide after being composted with cellulose. Ni/Cr-LDH increased surface area from 0.128 m^2/g to 2.207 m^2/g in Ni/Cr-C composites and Zn/Cr-LDH also increased in surface area from 0.133 m^2/g to 3.714 m^2/g in Zn/Cr-C composites. Based on these data, it can also be seen that Zn/Cr-LDH and Zn/Cr-C have a larger surface area than Ni/Cr-LDH and Ni/Cr-C. Based on the results of the characterization analysis of XRD, FT-IR, and BET, it is proven

Table 1. Data of BET Analysiss

Adsorbents	Surface Area (m^2/g)	Pore Volume (cm^3/g)	Pore Diameter (nm)
Ni/Cr-LDH	0.128	0.042	15.124
Zn/Cr-LDH	0.133	0.001	0.003
Ni/Cr-C	2.207	0.004	1.691
Zn/Cr-C	3.714	0.006	1.564

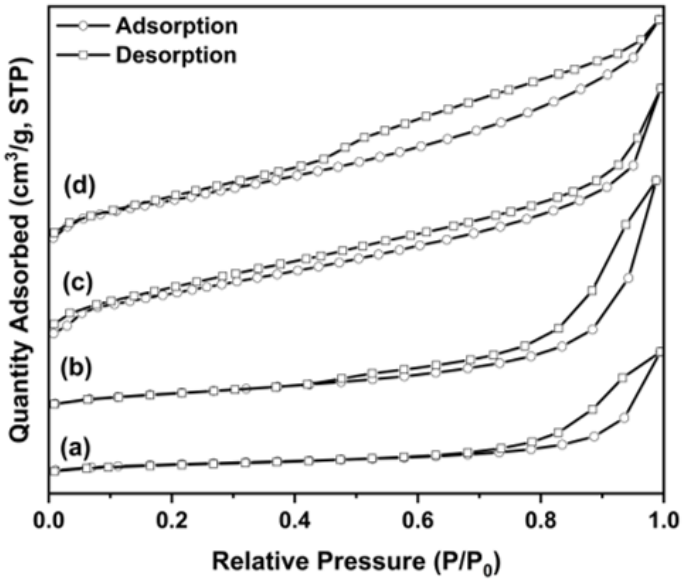

Figure 3. BET Profile of Ni/Cr-LDH (a), Zn/Cr-LDH (b), Ni/Cr-C (c), and Zn/Cr-C (e)

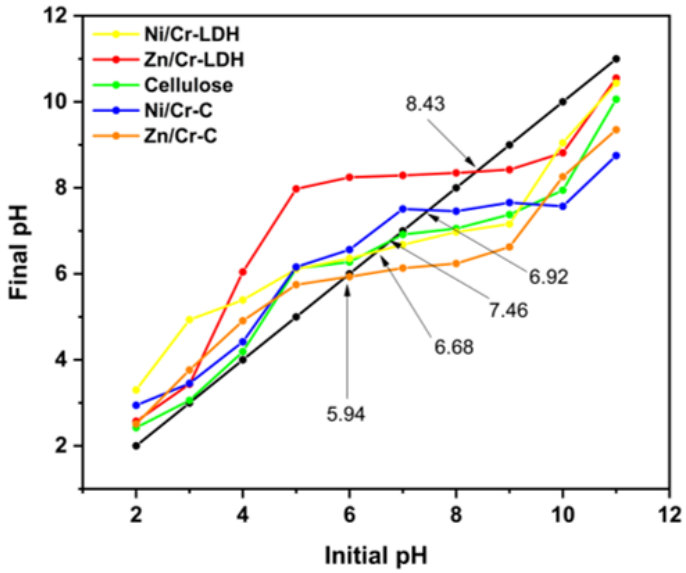

Figure 4. pH pzc of materials

that the preparation process of layered double hydroxide composites with cellulose has been successfully carried out, which is characterized by the emergence of peaks of diffraction of layered double hydroxide and cellulose in composite materials and an increase in surface area in composite materials.

The material in this study carried out a pHpzc test with the test results shown in Figure 4. Based on the results of the pH pzc test on each material, it is known that the pH pzc on materials Ni/Cr-LDH, Zn/Cr-LDH, cellulose, Ni/Cr-C, and Zn/Cr-C is 6.68, 8.43, 7.46, 6.92, and 5.94, respectively. Each material was also carried out a pH test in the phenol adsorption process to determine the optimum pH with the test results that can be seen in Figure 5. Based on Figure 5, it can be seen that the optimum pH of all materials in the phenol adsorption process is pH 9.

The materials were tested on the influence of adsorption contact time on the phenol adsorption process, which aims to determine the optimum adsorption time. Adsorption contact time was measured with a time variation of 0-180 minutes. Based on Figure 6, the equilibrium time of the adsorption process occurs at 70 minutes with an insignificant increase in adsorption concentration. Table 2 shows the adsorption kinet-

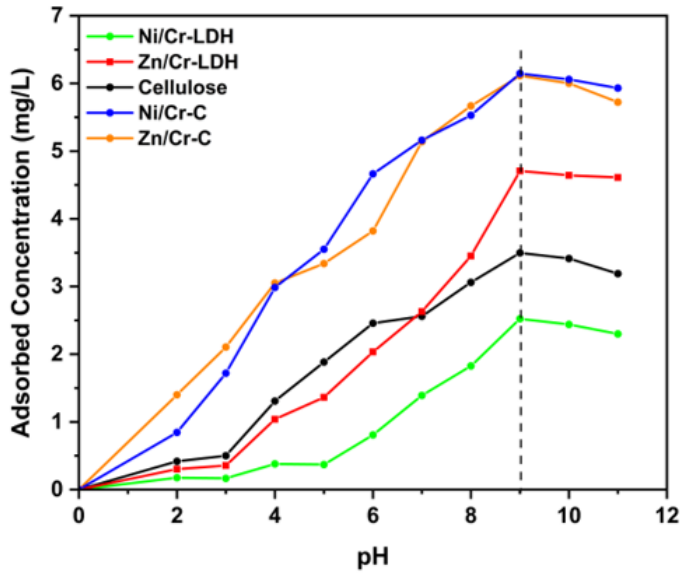

Figure 5. Effect of pH on Adsorption Process

Table 2. Adsorption Kinetic Parameters

Adsorbents	Initial Concentration (mg/L)	Qe_{exp} (mg/L)	Qe_{calc} (mg/L)	PFO R^2	k1	Qe_{calc} (mg/L)	PSO R^2	k2
Ni/Cr-LDH	10.059	2.616	1.935	0.959	0.034	2.846	0.998	0.026
Zn/Cr-LDH		4.100	3.755	0.927	0.045	4.627	0.988	0.013
Cellulose		3.618	1.684	0.904	0.032	3.798	0.999	0.035
Ni/Cr-C		5.167	3.178	0.969	0.037	5.495	0.999	0.019
Mg/Cr-C		6.058	5.261	0.946	0.046	6.780	0.992	0.009

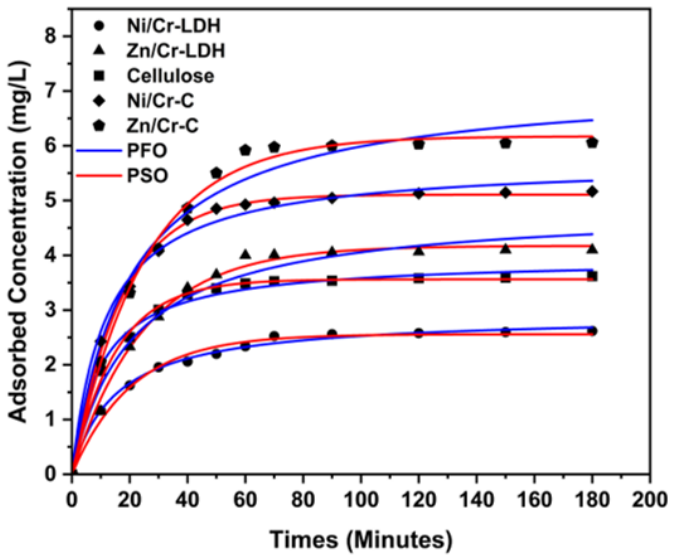

Figure 6. Adsorption Kinetic Models

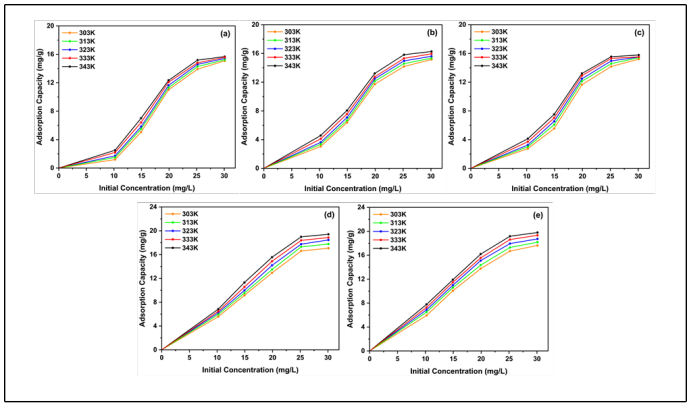

Figure 7. Effect of Initial Concentration and Temperature on Adsorption Process using Ni/Cr-LDH (a), Zn/Cr-LDH (b), Cellulose (c), Ni/Cr-C (d), and Zn/Cr-C (e)

ics followed by PSO through the value of the linear regression coefficient (R^2), close to the value of 1, and Qe_{calc} in PSO is closer to Qe_{exp} than in PFO.

Furthermore, each material was tested for the effect of initial concentration and temperature on the phenol adsorption process. Based on figure 7, it is known that the more the concentration and temperature increase, the adsorbed concentration also increases. From the test of the influence of the initial concentration and temperature that has been carried out can be determined isotherm and thermodynamic parameters with the results of the data shown in Tables 3 and 4. Based on Table 3, it can be seen that the adsorption capacity of each material where in Ni/Cr-LDH experienced an increase in adsorption capacity after becoming a Ni/Cr-C composite, from 8.985 mg/g to 24.510 mg/g, the same also happened in Zn/Cr-LDH experienced an increase in adsorption capacity from 13.263 mg/g to 30.960 mg/g. Based on Table 3, the Freundlich model is better than the Langmuir model for the adsorption process in this study, with the value of R^2 closer to the value of 1. This indicates that the adsorption process occurs multilayer. Based on Table 4, it can be seen that ΔG value overall shows negative values indicating a spontaneous adsorption process, ΔH value shows positively that the adsorption process is endothermic, with the enthalpy value in the 1.459–6.975 kJ/mol range indicating the physical adsorption process and ΔS shows degrees of irregularity.

The regeneration ability test on the material was also tested in this study to see the stability and effectiveness of the material. Based on figure 8, it can be seen that Ni/Cr-LDH and Zn/Cr-LDH materials can only be used repeatedly for 2^{nd} cycle while in Ni/Cr-C and Zn/Cr-C composite materials can survive the regeneration process until the 4^{th} cycle. this proves that the preparation process of LDH-cellulose composites can improve material performance in repeated use. A comparison of adsorption ability of phenol by several adsorbents can be seen in the Table 5. Based on Table 5, it can be seen that the adsorbent ability in Ni/Cr-C and Zn/Cr-C composite materials is superior to other adsorbents as evidenced by the large adsorption capacity and the optimum contact time, which is quite fast, which is 70 minutes. Figure 9 shows a plausible illustration of the M^{2+} difference on cellulose-based M^{2+}/Cr composite materials, where the use of M^{2+} with a larger atomic radius will affect the formation of interlayer space. The radius of atoms in M^{2+} or M^{3+} is larger, causing the appearance of a small interlayer space, and vice versa. It affects the adsorption ability of the material as evidenced by adsorption data where Zn/Cr-C composite material has a greater adsorption ability than Ni/Cr-C.

Table 3. Adsorption Isotherm Parameters

Adsorbents	Adsorption Isotherm	Adsorption Constant	Temperature 30°C	40°C	50°C	60°C	70°C
Ni/Cr-LDH	Langmuir	Qmax	2.055	2.968	3.893	6.146	8.985
		kL	0.063	0.061	0.058	0.053	0.048
		R^2	0.855	0.875	0.906	0.955	0.952
	Freundlich	n	0.238	0.275	0.306	0.365	0.412
		kF	2.424	2.066	1.862	1.608	1.472
		R^2	0.947	0.941	0.943	0.960	0.940
Zn/Cr-LDH	Langmuir	Qmax	9.606	13.263	6.382	7.380	6.135
		kL	0.046	0.041	0.101	0.111	0.173
		R^2	0.971	0.976	0.977	0.978	0.981
	Freundlich	n	0.446	0.498	0.539	0.602	0.686
		kF	35.530	17.923	11.130	6.206	3.388
		R^2	0.995	0.996	0.994	0.994	0.993
Cellulose	Langmuir	Qmax	6.925	9.542	13.245	7.097	8.110
		kL	0.051	0.046	0.041	0.102	0.112
		R^2	0.965	0.977	0.977	0.982	0.987
	Freundlich	n	0.407	0.456	0.503	0.588	0.653
		kF	13.868	11.150	10.495	7.244	4.383
		R^2	0.999	0.999	0.997	0.997	0.998
Ni/Cr-C	Langmuir	Qmax	24.450	24.510	24.510	23.095	22.676
		kL	0.189	0.227	0.278	0.428	0.601
		R^2	0.886	0.902	0.950	0.972	0.984
	Freundlich	n	0.784	0.847	0.892	1.000	1.126
		kF	1.946	1.377	1.057	1.386	1.989
		R^2	0.912	0.910	0.943	0.939	0.937
Zn/Cr-C	Langmuir	Qmax	30.960	28.571	27.100	26.525	25.381
		kL	0.116	0.161	0.218	0.277	0.386
		R^2	0.856	0.909	0.918	0.941	0.958
	Freundlich	n	0.848	0.969	1.097	1.201	1.394
		kF	1.363	1.157	1.699	2.227	3.121
		R^2	0.961	0.966	0.979	0.970	0.983

Table 4. Adsorption Thermodynamic Parameters

Adsorbents	Concentration (mg/L)	T (K)	Qe (mg/g)	△H (kJ/mol)	△S (J/mol. K)	△G (kJ/mol)
Ni/Cr-LDH	30.082	303	15.078	1.794	0.006	-0.011
		313	15.226			-0.070
		323	15.412			-0.130
		333	15.579			-0.190
		343	15.681			-0.249
Zn/Cr-LDH	30.082	303	15.152	3.275	0.011	-0.012
		313	15.338			-0.121
		323	15.607			-0.229
		333	15.950			-0.338
		343	16.275			-0.446
Cellulose	30.082	303	15.208	1.459	0.005	-0.060
		313	15.403			-0.111
		323	15.495			-0.161
		333	15.523			-0.211
		343	15.783			-0.261
Ni/Cr-C	30.082	303	17.072	6.975	0.025	-0.698
		313	17.768			-0.952
		323	18.455			-1.205
		333	18.863			-1.458
		343	19.410			-1.711
Zn/Cr-C	30.082	303	17.629	6.698	0.025	-0.862
		313	18.176			-1.112
		323	18.724			-1.361
		333	19.327			-1.611
		343	19.790			-1.860

Table 5. Regeneration Ability of Materials

Adsorbents	Adsorption Capacity (mg/g)	Optimum Contact Time	References
Date palm fibers	19.57	24 hours	(Alminderej et al., 2022)
Natural clays	10	2 hours	(Dehmani et al., 2021)
Moroccan clay	15.11	2,5 hours	(Dehmani et al., 2020)
Fe_3O_4/chitosan/ZIF-8 nanocomposit	6.43	40 minutes	(Keshvardoostchokami et al., 2021)
Hematite iron oxide nanoparticles	5.35	2 hours	(Dehbi et al., 2020)
Activated carbon from palm kernel shell	23.82	-	(Hernández-Barreto et al., 2020)
Unactivated Moringa oleifera Seed Shells residue	6.95	-	(Sani et al., 2020)
Aluminum oxide nanoparticles	16.97	-	(Safwat et al., 2022)
Banana Peels Activated Carbon	6.98	1 hour	(Ingole et al., 2017)
Biochar from the pine fruit shells (BC550)	26.738	1 hour	(Ingole et al., 2017)
Rice Husk Activated Carbon	28	-	(Mohammad et al., 2014)
Diethylenetriamine modified activated carbon	18.12	-	(Saleh et al., 2018)
Zn_4Al-LDH	23.4	1 hour	(Lupa et al., 2018)
Ni/Cr-C	24.51	70 minutes	This study
Zn/Cr-C	30.96	70 minutes	This study

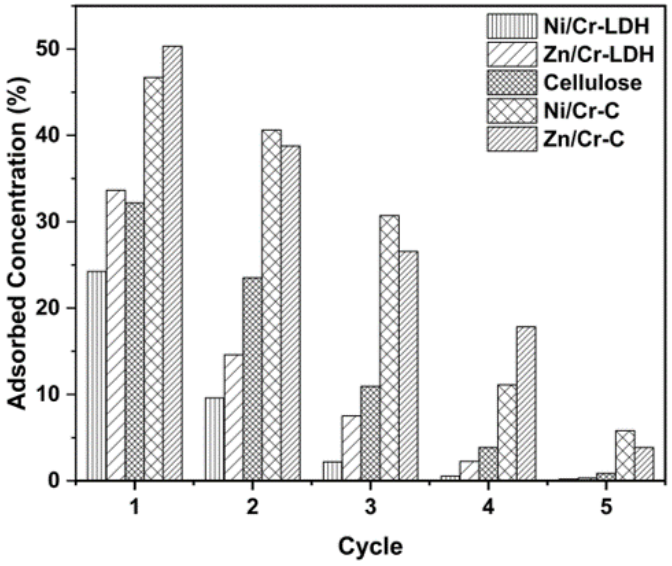

Figure 8. Regeneration Ability of Materials

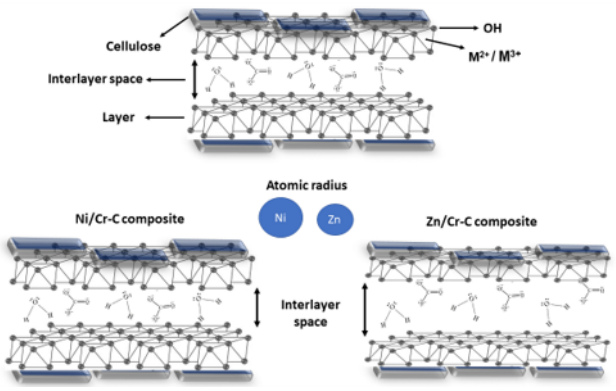

Figure 9. Plausible Illustration of M^{2+} Difference on Cellulose-based M^{2+} /Cr Composite

4. CONCLUSION

Ni/Cr-C and Zn/Cr-C composite materials have been successfully carried out, as evidenced by XRD, FTIR, BET analysis, increased surface area, adsorption ability, and regeneration ability. Ni/Cr-C and Zn/Cr-C composite materials can be used repeatedly on the regeneration process until the 4^{th} cycle. Based on adsorption data, Zn/Cr-C composite material has a greater adsorption ability than Ni/Cr-C. Kinetic and isotherm model in this study followed by PSO kinetic and Freundlich isotherm.

5. ACKNOWLEDGMENT

The authors thank to Research Center of Inorganic Materials and Coordination Complexes, Faculty of Mathematics and Natural Sciences, Sriwijaya University for support and instrumental analysis.

REFERENCES

Alminderej, F. M., A. M. Younis, A. E. Albadri, W. A. El-Sayed, Y. El-Ghoul, R. Ali, A. M. Mohamed, and S. M. Saleh (2022). The Superior Adsorption Capacity of Phenol from Aqueous Solution Using Modified Date Palm Nanomaterials: A performance and Kinetic Study. *Arabian Journal of Chemistry*, **15**(10); 104120

Chaghaganooj, Z. D., N. Asasian-Kolur, S. Sharifian, and M. Sillanpää (2021). Ce and Mn/bio-waste-based Activated Carbon Composite: Characterization, Phenol Adsorption and Regeneration. *Journal of Environmental Chemical Engineering*, **9**(4); 105788

da Silva, M. C., C. Schnorr, S. F. Lütke, S. Knani, V. X. Nascimento, É. C. Lima, P. S. Thue, J. Vieillard, L. F. Silva, and G. L. Dotto (2022). KOH Activated Carbons from Brazil Nut Shell: Preparation, Characterization, and Their Application in Phenol Adsorption. *Chemical Engineering Research and Design*, **187**; 387–396.

Debnath, B., P. Duarah, D. Haldar, and M. K. Purkait (2022). Improving the Properties of Corn Starch Films for Applica-

tion as Packaging Material Via Reinforcement with Microcrystalline Cellulose Synthesized from Elephant Grass. *Food Packaging and Shelf Life*, **34**; 100937

Dehbi, A., Y. Dehmani, H. Omari, A. Lammini, K. Elazhari, S. Abouarnadasse, and A. Abdallaoui (2020). Comparative Study of Malachite Green and Phenol Adsorption on Synthetic Hematite Iron Oxide Nanoparticles (α-Fe2O3). *Surfaces and Interfaces*, **21**; 100637

Dehmani, Y., D. Dridi, T. Lamhasni, S. Abouarnadasse, R. Chtourou, and E. C. Lima (2022). Review Of Phenol Adsorption On Transition Metal Oxides And Other Adsorbents. *Journal of Water Process Engineering*, **49**; 102965

Dehmani, Y., O. El Khalki, H. Mezougane, and S. Abouarnadasse (2021). Comparative Study on Adsorption of Cationic Dyes and Phenol by Natural Clays. *Chemical Data Collections*, **33**; 100674

Dehmani, Y., L. Sellaoui, Y. Alghamdi, J. Lainé, M. Badawi, A. Amhoud, A. Bonilla-Petriciolet, T. Lamhasni, and S. Abouarnadasse (2020). Kinetic, Thermodynamic and Mechanism Study of the Adsorption of Phenol on Moroccan Clay. *Journal of Molecular Liquids*, **312**; 113383

Dong, F.X., L. Yan, X.H. Zhou, S.T. Huang, J.Y. Liang, W.X. Zhang, Z.W. Guo, P.-R. Guo, W. Qian, L.-J. Kong, et al. (2021). Simultaneous Adsorption of Cr (VI) and Phenol by Biochar-based Iron Oxide Composites in Water: Performance, Kinetics and Mechanism. *Journal of Hazardous Materials*, **416**; 125930

Gao, W., Z. Lin, H. Chen, S. Yan, H. Zhu, H. Zhang, H. Sun, S. Zhang, S. Zhang, and Y. Wu (2022). Roles of Graphitization Degree and Surface Functional Groups of N-doped Activated Biochar for Phenol Adsorption. *Journal of Analytical and Applied Pyrolysis*, **167**; 105700

Hernández-Barreto, D. F., L. Giraldo, and J. C. Moreno-Piraján (2020). Dataset on Adsorption of Phenol Onto Activated Carbons: Equilibrium, Kinetics and Mechanism Of Adsorption. *Data in Brief*, **32**; 106312

Ingole, R. S., D. H. Lataye, and P. T. Dhorabe (2017). Adsorption of Phenol Onto Banana Peels Activated Carbon. *KSCE Journal of Civil Engineering*, **21**(1); 100–110

Juleanti, N., N. R. Palapa, T. Taher, N. Hidayati, B. I. Putri, and A. Lesbani (2021). The Capability of Biochar-based CaAl and MgAl Composite Materials as Adsorbent for Removal Cr (VI) in Aqueous Solution. *Science and Technology Indonesia*, **6**(3); 196–203

Keshvardoostchokami, M., M. Majidi, A. Zamani, and B. Liu (2021). Adsorption of Phenol on Environmentally Friendly Fe_3O_4/Chitosan/Zeolitic Imidazolate Framework-8 Nanocomposite: Optimization by Experimental Design Methodology. *Journal of Molecular Liquids*, **323**; 115064

Liu, J., J. Li, X. Bing, D. H. Ng, X. Cui, F. Ji, and D. D. Kionga (2018). ZnCr-LDH/N-Doped Graphitic Carbon-incorporated g-C_3N_4 2D/2D Nanosheet Heterojunction with Enhanced Charge Transfer for Photocatalysis. *Materials Research Bulletin*, **102**; 379–390

Lupa, L., L. Cocheci, R. Pode, and I. Hulka (2018). Phenol Adsorption using Aliquat 336 Functionalized Zn-Al Layered Double Hydroxide. *Separation and Purification Technology*, **196**; 82–95

Mohammad, Y., E. Shaibu-Imodagbe, S. Igboro, A. Giwa, and C. Okuofu (2014). Adsorption of Phenol from Refinery Wastewater Using Rice Husk Activated Carbon. *Iranian (Iranica) Journal of Energy & Environment*, **5**(4)

Padalkar, N. S., S. V. Sadavar, R. B. Shinde, A. S. Patil, U. M. Patil, D. S. Dhawale, R. N. Bulakhe, H. Kim, H. Im, A. Vinu, et al. (2022). Layer-by-layer Manohybrids of Ni-Cr-LDH Intercalated with 0D Polyoxotungstate for Highly Efficient Hybrid Supercapacitor. *Journal of Colloid and Interface Science*, **616**; 548–559

Safwat, S. M., N. Y. Mohamed, M. N. Meshref, and A. Elawwad (2022). Adsorption of Phenol onto Aluminum Oxide Nanoparticles: Performance Evaluation, Mechanism Exploration, and Principal Component Analysis (PCA) of Thermodynamics. *Adsorption Science & Technology*, **2022**

Sahu, J., R. R. Karri, and N. Jayakumar (2021). Improvement in Phenol Adsorption Capacity On Eco-friendly Biosorbent Derived From Waste Palm-oil Shells Using Optimized Parametric Modelling of Isotherms and Kinetics by Differential Evolution. *Industrial Crops and Products*, **164**; 113333

Saleh, T. A., S. O. Adio, M. Asif, and H. Dafalla (2018). Statistical Analysis of Phenols Adsorption on Diethylenetriamine-modified Activated Carbon. *Journal of Cleaner Production*, **182**; 960–968

Sani, D. E., J. O. Idoko, E. S. Okwute, and M. C. Apeh (2020). Adsorption of Phenol Onto Unactivated Moringa Oleifera Seed Shells Residue by UV-visible Spectrophotometer. *GSC Biological and Pharmaceutical Sciences*, **13**(2); 080–090

Sun, J., Y. Wang, Y. He, J. Liu, L. Xu, Z. Zeng, Y. Song, J. Qiu, Z. Huang, and L. Cui (2022). Effective Removal of Nanoplastics from Water by Cellulose/MgAl Layered Double Hydroxides Composite Beads. *Carbohydrate Polymers*, **298**; 120059

Ullah, N., Z. Ali, S. Ullah, A. S. Khan, B. Adalat, A. Nasrullah, M. Alsaadi, and Z. Ahmad (2022). Synthesis of Activated Carbon-surfactant Modified Montmorillonite Clay-alginate Composite Membrane for Methylene Blue Adsorption. *Chemosphere*; 136623

Wang, X., B. Cheng, L. Zhang, J. Yu, and I. Normatov (2022). Adsorption Performance of Tetracycline on NiFe Layered Double Hydroxide Hollow Microspheres Synthesized with Silica as the Template. *Journal of Colloid and Interface Science*, **627**; 793–803

Yuliasari, N., Badri, A. F., Wijaya, A., Mega, P., Bahar, S., Siregar, N., and Mohadi, R. (2022). Modification of Mg/Al-LDH Intercalated Metal Oxide (Mg/Al-Ni) to Improve the Performance of Methyl Orange and Methyl Red Dyes Adsorption Process. *Science and Technology Indonesia*, **7**(3); 275–283

